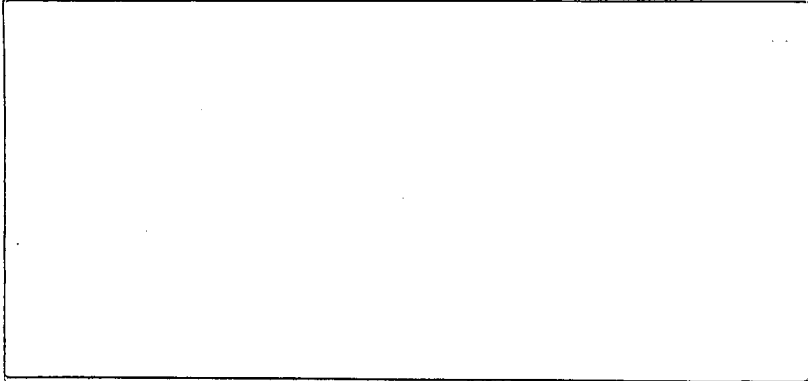


Docket # 50-286
Control # 8407020425
Date 6/25/84 Document:
REGULATORY DOCKET FILE



— NOTICE —

THE ATTACHED FILES ARE OFFICIAL RECORDS OF THE DIVISION OF DOCUMENT CONTROL. THEY HAVE BEEN CHARGED TO YOU FOR A LIMITED TIME PERIOD AND MUST BE RETURNED TO THE RECORDS FACILITY BRANCH 016. PLEASE DO NOT SEND DOCUMENTS CHARGED OUT THROUGH THE MAIL. REMOVAL OF ANY PAGE(S) FROM DOCUMENT FOR REPRODUCTION MUST BE REFERRED TO FILE PERSONNEL.

DEADLINE RETURN DATE	_____
_____	_____
_____	_____
_____	_____

RECORDS FACILITY BRANCH

New York Power Authority Contract No. 80-121

Final Report, August 5, 1983
Revision 1, September 28, 1983

Report Number 83-105

DEVELOPMENT OF MATERIAL PROPERTY DATA
FOR THE TEARING STABILITY ANALYSIS OF THE
INDIAN POINT 3 PRIMARY COOLANT SYSTEM

Prepared by

FRACTURE PROOF DESIGN CORPORATION
77 Maryland Plaza
St. Louis, MO 63108

Principal Investigators

K. H. Cotter
Paul C. Paris
Farough Baradari

Prepared for

New York Power Authority
123 Main Street
White Plains, NY 10601

New York Power Authority Project Manager

James V. Brunetti
Civil-Structural Department, Design and Analysis

(NON-PROPRIETARY)

8407020471 840625
PDR ADOCK 05000286
PDR
P

ABSTRACT

For the past decade, tough materials have been characterized by the use of the J-integral crack growth resistance curve or J-R curve. Early J-R curve tests were limited to small crack extensions because the usual purpose of the tests was to determine the fracture toughness of the material, i.e., a J_{Ic} value. Such tests were valid for their intended purposes. After the development of plastic tearing stability concepts, the need for material characterization at values of J and crack extension, Δa , above J_{Ic} was obvious. In order to apply tearing stability methods to the analysis of cracks in nuclear reactor piping, data for very high values of J and large Δa are required. Furthermore, the tests must meet J-controlled growth criteria which was absent in a number of earlier tests.

In this paper, tests of typical stainless steels used in primary coolant system piping of PWR and BWR reactors are presented. The parameters considered in the test program included: temperature, 70F vs. 550F; side grooving; Inconel vs. stainless weld metal; cast vs. wrought product form; and, the location of the crack in either the base metal or in the weld metal. These parameters were evaluated in tests for values of J up to 50,000 in-lb/in² and Δa up to 5 inches.

The results are presented in the form of J vs. T stability curves. It was shown that the heretofore use of wrought stainless steel data based on small crack extensions and low J values is unconservative. The development of this new data suggests that certain of the analyses of nuclear piping that have been performed to date must be re-evaluated and, specifically, that the strong dependence of the material tearing resistance on the magnitude of the applied J must be taken into account.

INTRODUCTION

The objective of this study was to develop material property data in the form of tearing resistance curves or J_{mat} vs. T_{mat} . J_{mat} values in the vicinity of 50-60,000 in-lb/in². Furthermore, the material property data had to be representative of forged stainless pipe, cast stainless elbows and several weld types over a temperature range from 70F to 550F as is found in typical BWR and PWR piping.

SPECIMEN DESIGN

Prior to the initiation of this program, the typical approach to developing J-R curves was to use a 1T or 2T compact tension (CTS) type of specimen design. The limitation in the utilization of a 1T or 2T specimen is that the maximum obtainable value of the J-integral tends to be considerably less than is required by this project. A further limitation stems from the requirement that the test data be within the allowable limits for J-controlled growth which is typically governed by the value of ω . The physical limitation imposed by the ω limits is that the crack extension, Δa , that is permitted for the 1T or 2T type specimen tends to be small. This follows from the ratio of the Δa to the remaining ligament, b. In order to

circumvent this problem, a modified CTS design was used with dimensions $B = 1.0$ and $W = 20.0$ inches. This specimen is basically a modification of the standard CTS design that permits achieving large crack extension Δa and high values of J .

Another feature of the specimen design was that the specimen could be reused for developing J-R curves for welds. This eliminated the need to fabricate additional specimens for weld material thereby keeping the test program costs as low as possible. The initial specimen design assumed that the test parameters would require the use of $a/W = .6$ to $.7$. Although it was not originally intended, it was decided early in the test program that buckling guides would be required because the deformation of the specimen induced out-of-plane bending moments that could result in buckling and thereby invalidate the test. The specimen was also selected so that the compliance method for determining Δa , that is used for the smaller CTS specimens, could be directly extended to this size specimen.

MATERIALS

A number of the PWR and BWR nuclear reactor primary cooling system (RCS) piping systems are fabricated from A376, TP316 forged sections and A351, Grade CF8M cast elbows. Thus, these materials were identified as being representative and could serve as the basis for this project. As no piping or elbow sections of actual piping were readily available at reasonable cost, suitable substitutes were required.

A240 Plate

Typical piping sizes range up to 36 inches in diameter with wall thickness up to 2.5 inches. Upon review of the material specifications for A376, TP316 piping, it was determined that a suitable substitute would be A240, TP316 plate. The one-inch thickness was selected based on cost considerations and to facilitate ease in handling the specimens. Based on a review of the existing (through 1981) literature, it was determined that data based on one-inch thick material would not be significantly different from the actual wall thicknesses found in the piping.

CF8M Cast Plate

The actual elbows found in the in RCS are cast CF8M, TP316 stainless steel. The ID's of the elbows range from 27.5 to 31 inches and have wall thicknesses that range from 2.56 to 2.88 inches. As with the piping, there were no elbows available at affordable prices and it was necessary to develop representative material for use in the specimens. One approach considered was that of making centrifugally or statically cast pipe sections, slitting the sections, and then rolling them flat to make a specimen suitable for testing. This was rejected in favor of a static cast flat plate. This casting design used simulated cooling rates that might be expected in the actual elbow castings.

The soundness requirement used for casting of the plate was that one of the four quadrants of the plate had to meet the radiography requirements of ASTM E-446, Severity Level 2. It was further mandated that the best quadrant meeting Level 2 or better should be identified as that would be the quadrant that would be used for developing material property data.

Welds

After testing the base metal specimens, the specimens were cut into two pieces along the plane of fracture. Thus, the specimens for welding were obtained by re-using these A240 and CF8M base metal test specimens. Then, the outside edges of the plate (the edges parallel to the fracture plane) were bevelled in preparation for welding. Welds were then made using both E316L electrodes and Inconel weld metal. The following welds were made: E316L weld of A240 plate, E316L weld of CF8M cast plate, and Inconel weld of A240 plate.

It is important to note that the actual welding of the specimens was performed by welders that are qualified for fabrication at a nuclear plant construction site. Thus, the conditions surrounding the fabrication of the specimens were as close as possible to the typical conditions existing during the fabrication of a plant rather than that of a laboratory environment.

TEST PROCEDURE

The specimens were finish-machined followed by saw cutting to a pre-determined length to facilitate pre-cracking. A pre-cracking procedure following ASTM E813-81(1) was utilized to produce a crack having the desired initial length. The test was conducted following the procedures of ASTM E813-81(1) and periodic unloading slopes were produced following the usual procedures. The load was measured by a load cell and recorded both digitally and graphically. The displacement was computed based on the measured ram stroke and was recorded both digitally and graphically. Verification of crack extension, Δa , was achieved using optical observation of crack extension and fatigue marker bands. In addition, the final crack length was compared with the predicted crack length.

DATA REDUCTION

Preliminary data in the form of J vs. Δa was derived. But, data, in the form of J - Δa curves, cannot be readily adapted for use in analytical studies of crack stability. Accordingly, development of J - T curves is required. Because the preliminary data contained some scatter, smoothing was required. The procedures for smoothing of the data, plotting, correcting for errors in Δa based on observed vs. computed and correcting for displacement effects on J and Δa follow below.

Smoothing

As mentioned above, the raw laboratory data contained varying degrees of scatter, that is normally found, along with errors due to large displacement effects. The effects of large displacement were accounted for by introducing a correction due to Tada(2). Then, using a conservative procedure, the data was smoothed. The conservatism in the approach included the developing of an adjusted or smoothed J- Δa curve wherein the value of J, as adjusted, and the slope of the smoothed J- Δa curve are always less than what is evident from the actual corrected experimental data. It must be emphasized that the purpose for this smoothing is simply to facilitate the numerical computation of dJ/da from the data by the computer codes. That is, data containing the usual amount of scatter does not lend itself readily to development of tearing modulus values.

Development of $J_{mat}-T_{mat}$ Curves

The J- Δa curves, after smoothing, were used to develop $J_{mat}-T_{mat}$ curves for each of the test conditions. The method used relied on fitting a second order polynomial through five points and taking the slope at the mid-point. This procedure and plotting of the data was achieved using the JTPlot(4) program.

FRACTURE SURFACE MORPHOLOGY

Figure 1 compares the fracture surfaces of A240 plate tests. The specimens are numbered from left to right, starting with specimens SS4 and SS6 which were tested at 70F and followed by specimens SS3, SS7 and SS8 which were all tested at 550F. It is noted that there is considerably more shear on the specimens at 550F compared with those at 70F. However, this is not true for the specimen with side-grooving, SS8, where a very flat fracture surface is noted.

The cast CF8M material at the two temperatures is shown in Figure 2. On the left side of the figure, the 550F specimens C2 and C4 are shown followed by C3 and C1 at 70F. In comparing the cast fracture surfaces with those of the A240 plate, it is noted that the fracture surface is much more granular in appearance and that there is considerable deformation evident on the side of the specimen. It is further noted that the elevated temperature specimens tend to have slightly more shear on the fracture surface than at 70F.

The pronounced difference between the cast vs. wrought fracture surfaces can be seen in Figure 3. The specimens on the left are cast specimens C4 and C2 followed by wrought specimens SS3 and SS7 and all were tested at 550F.

The welded cast specimens are shown in Figure 4 wherein we read from left to right as follows: the first specimen is WC1, followed by WC4, WC3, WC2, then followed by the unwelded specimens, C4 and C2. All of these specimens were tested at 550F. We further note that specimen WC1 had been side-grooved and shows a much flatter fracture surface than the other specimens. As might be expected, the fracture surfaces of the welds are quite similar to that of the cast specimens.

The welded plate specimens, again from 550F tests, are shown in Figure 5. The side-grooved specimen, on the far left, is WSS4 and it shows a very flat fracture surface. This is followed by three other welded specimens, WSS7, WSS6 and WSS3. Lastly, the unwelded specimens SS3 and SS7 are shown on the right-hand side of Figure 5. It is noted that the fracture surface of welded plate specimens tends to be quite similar to that of the unwelded specimens. It is also noted, by comparing Figures 4 and 5, that the appearance of the fracture surface of the welded cast plate shows considerable difference from the welded plate.

Finally, in Figure 6 we compare the Inconel weld with the E316L weld. Reading from left to right, we have specimen WSS7 followed by WSS2, WSS4 and finally WSS1. The two specimens on the right are side-grooved and show a much flatter fracture surface than those which are not. Specimens WSS1 and WSS2 are from an Inconel weld while the others are from the E316L weld and all were tested at 550F.

TEARING RESISTANCE RESULTS

Base Metal

Figure 7 shows the crack growth resistance data developed for A240 plate. No predominant temperature effect can be seen upon comparing the 70F and 550F tests. However, the side-grooving naturally lowers the value of the tearing modulus for corresponding values of J.

On the contrary, a pronounced temperature effect is found to exist for cast CF8M as seen in Figure 8. This effect is consistent with the results of Bamford and Bush(3) and other investigators(5-7). In comparing the difference between cast and wrought type 316 stainless steel, as shown in Figures 9, it is noted that the cast material has lower tearing resistance at 550F than that for the A240 plate.

The actual effect of the side-groove can be idealized as follows. Since the actual pipe does not contain a side-groove, rather it is either smooth or has a weld, there is no need to use test data based on the side-groove for an application that does not involve a side-groove. It is noted that side-grooving may be a reasonable idealization of the behavior of cracks in the presence of IGSCC such as that found in BWR recirculation piping. However, PWR primary systems are not prone to IGSCC. Thus, it is felt that utilization of data based on side-grooving may be unduly conservative for applications not prone to IGSCC. Side-grooving, however, does serve to keep the crack growth along a well-defined plane as can be noted by observing the fracture surfaces. Therein it is readily apparent that the side-grooved specimens result in a very flat crack plane whereas the others tend to seek the path of least resistance.

Weld Metal

In Figure 10, welded A240 plate is compared with base metal. Therein it is readily apparent that the welds have properties that tend to be quite

similar to those of the base metal. This is noted by comparing specimens SS3 and SS7 with WSS3 and WSS7. We note that specimens SS8 and WSS4 are side-grooved which accounts for their lower tearing resistance. The results for specimen WSS6 were considered an anomaly. This conclusion can be drawn by observing Figure 5 wherein the crack surface morphology of specimen WSS6 is characteristically different from those of the other welded A240 specimens. Specimen WSS6 will be subjected to fractography and metallurgical evaluation in the future to attempt to isolate the causative metallurgical factors. The similarity of the crack surface morphology of the base metal specimens SS3 and SS7 with the welded specimens WSS3 and WSS7 should be noted. It is reasonable to use the same argument to disregard the side-grooved WSS4 data as was used for the SS8 side-grooved specimens.

In Figure 4, the similarity of the crack surface morphology of the welded CF8M with the base metal CF8M can be noted. This would lead to the expectation of similar resistance curves for the welded CF8M compared with the CF8M base metal. However, some noticeable difference occurs upon examining the values of the tearing modulus. The results shown in Figure 11 indicate that the tearing resistance of the weld specimens is less than the base metal. This can be attributed to the difference in flow stress between the weld and base metals.

Finally, in Figure 12, the results of the Inconel weld tests on specimens WSS1 and WSS2 are compared with those of the E316L welds. It is noted that very little difference exists between the two types of welds. The specimens without the side-grooves, WSS2, WSS3 and WSS7, have similar tearing resistance. For the specimens with the side-grooves, WSS1 and WSS4, the tearing resistances are quite similar with the Inconel data showing slightly greater resistance.

Lower Bound Data

The development of lower bound crack growth resistance data must be based on both the crack driving force, J_{mat} , and the value of the tearing modulus, T_{mat} . A complete set of all tests is shown in Figure 13. It is immediately apparent that the side-grooved welded specimens WSS4 and WC1 have the lowest values. As stated before, it is not felt that this data is representative of the conditions that are present in PWR's not prone to IGSCC. Upon further examination, the data evidenced by specimens WC4 and WSS7 appear to represent valid lower bounds for the cast and wrought material respectively in non-IGSCC environments.

CONCLUSIONS

It was shown that a definite temperature dependence exists for a wide range of J_{mat} values for cast CF8M stainless steel. It was also shown that welds have lower tearing resistance than base metal and that side-grooving can reduce the apparent crack growth resistance properties of both base metal and weld metal material. It was concluded that use of tearing modulus data based on cast CF8M at 550F is a reasonable lower bound for most stainless steel piping applications. This lower bound is strictly applicable only to welds of cast sections. Stability can be demonstrated for higher values of

applied tearing modulus in wrought than in cast TP316 stainless steels and similarly in base than in weld metals.

Based on the above results, we find an overall minimum expected value for tearing modulus to be approximately 20 at 550F in a CF8M weldment and at a value of J_{mat} equal to 28,000. Somewhat higher values of T_{mat} are found for other materials.

Such results suggest that previous analyses of stainless steel piping that were based on values of $T_{mat} = 200$ must be re-evaluated to insure structural safety is not impaired.

REFERENCES

1. ASTM Specification E813-81.
2. Tada, Hiroshi, Private Communication, April 1983.
3. "Fracture Behavior of Stainless Steel", Bamford, W. H. and Bush, A. J., ASTM STP 668, p. 553, 1979.
4. "JIPILOT" Computer Code, Version 2, Level 3, Fracture Proof Design Corporation, St. Louis, MO.
5. Private Communication, John Gudas, NSRDC, Annapolis, MD, July 1981.
6. "The Effect of Aging on Cast Stainless Steel", Bamford, W.H., Westinghouse Report dated June 1980.
7. "Interim Report on Fracture Toughness of Operating Reactor Internal Stress", James, L.A., HEDL Corr. No. 7950722, dated March 1, 1979.

Table 1, SUMMARY OF TEST PARAMETERS

Spec. No.	Material	a_i/W	Temp(F)	Side Grooved
SS4	A240 plate	.693	70	N
SS6	"	.604	70	N
SS3	"	.696	550	N
SS7	"	.603	550	N
SS8	"	.675	550	Y
C1	CF8M cast	.601	70	N
C3	"	.602	70	N
C2	"	.606	550	N
C4	"	.603	550	N
WSS1	Inconel weld (A240)	.600	550	Y
WSS2	"	.590	550	N
WSS3	E316 weld (A240)	.590	550	N
WSS4	"	.600	550	Y
WSS6	"	.600	550	N
WSS7	"	.585	550	N
WC1	E316L weld (CF8M)	.595	550	Y
WC2	"	.595	550	N
WC3	"	.600	550	N
WC4	"	.590	550	N

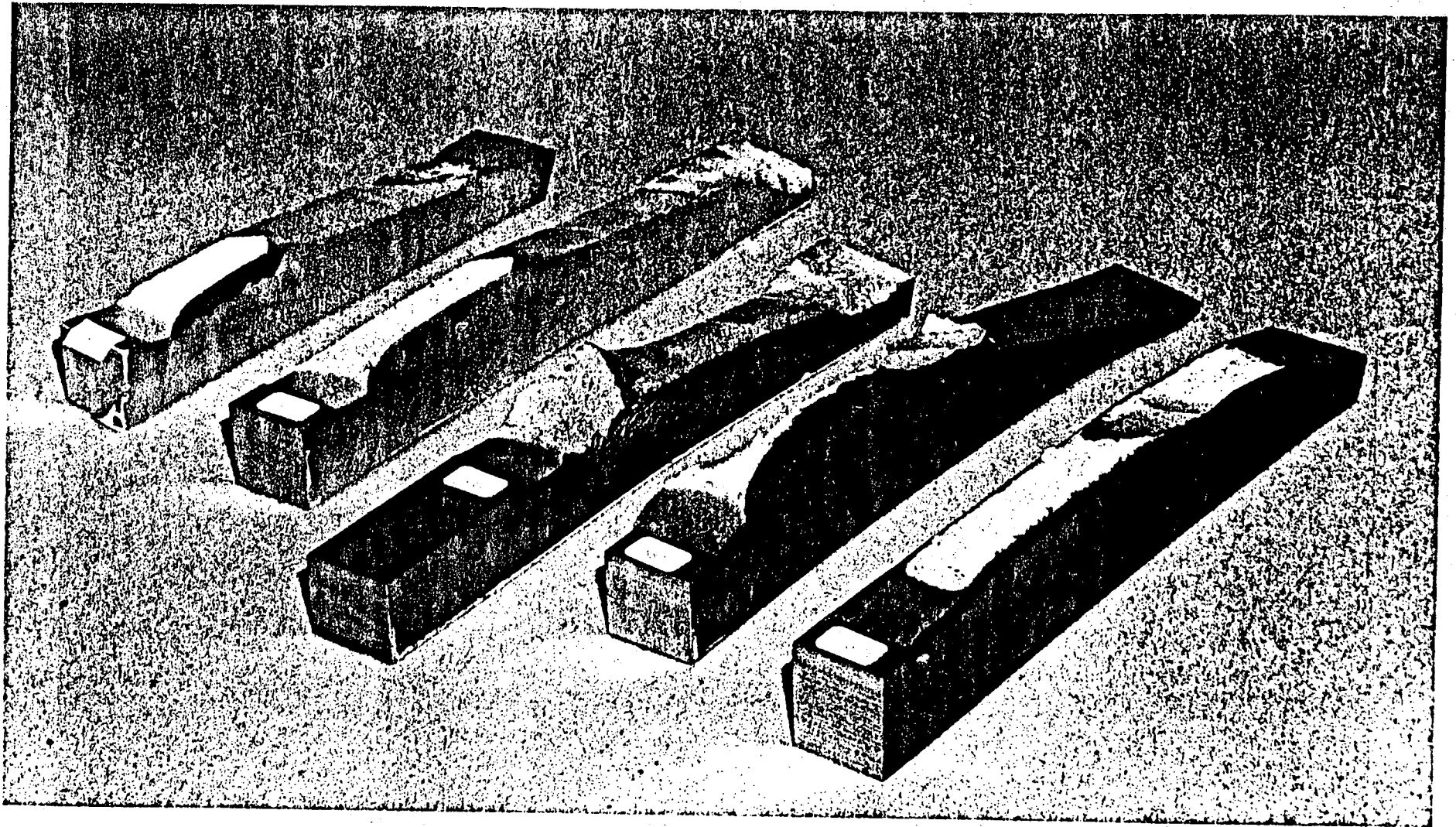


Figure 1 Fracture Surfaces of A240 Plate Test Specimens. Specimens
Numbered Left to Right: SS4, SS6, SS3, SS7, SS8

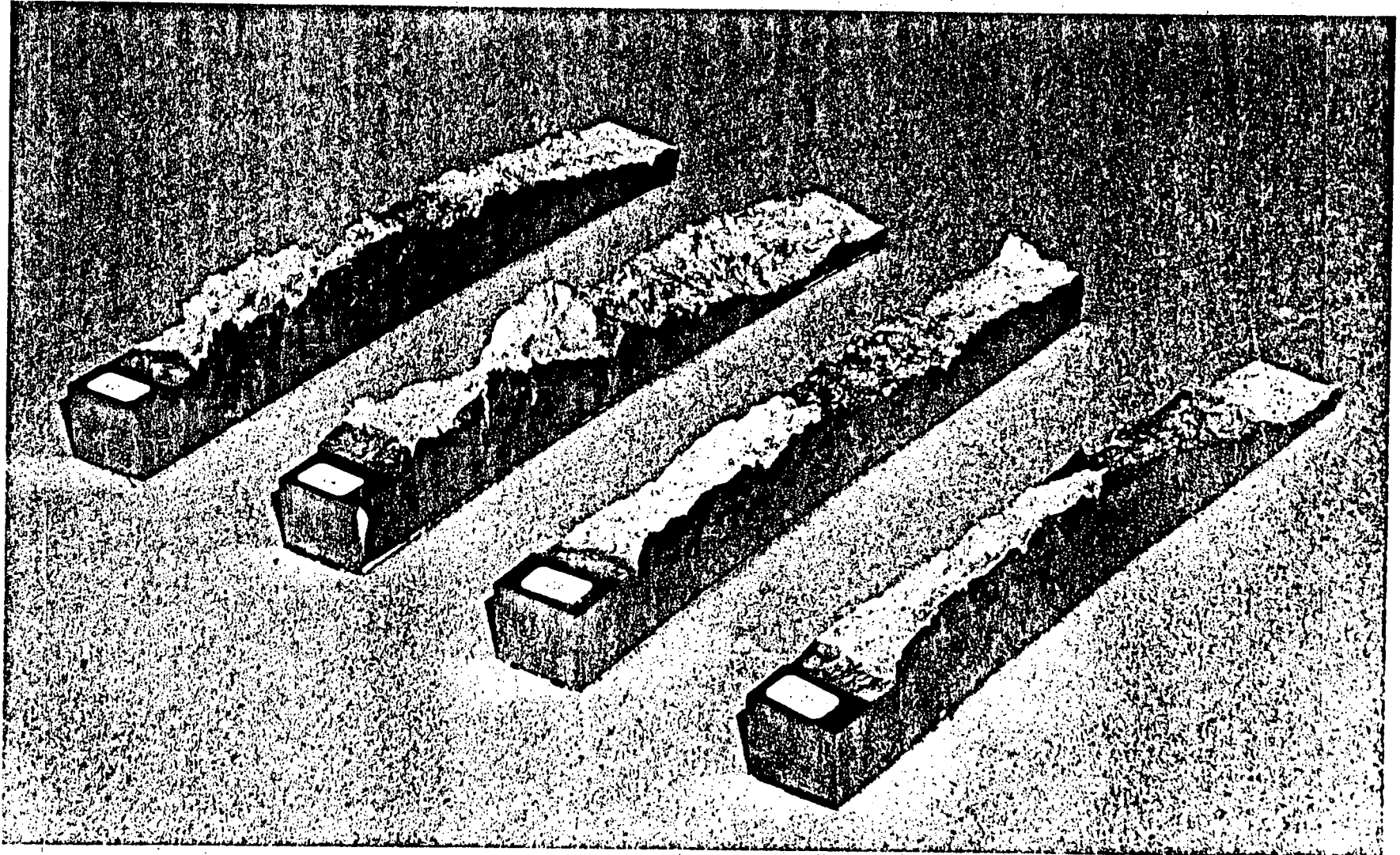


Figure 2 Cast CF8M Test Specimen Fracture Surfaces. Specimens Numbered
Left to Right: C2, C4, C3, C1

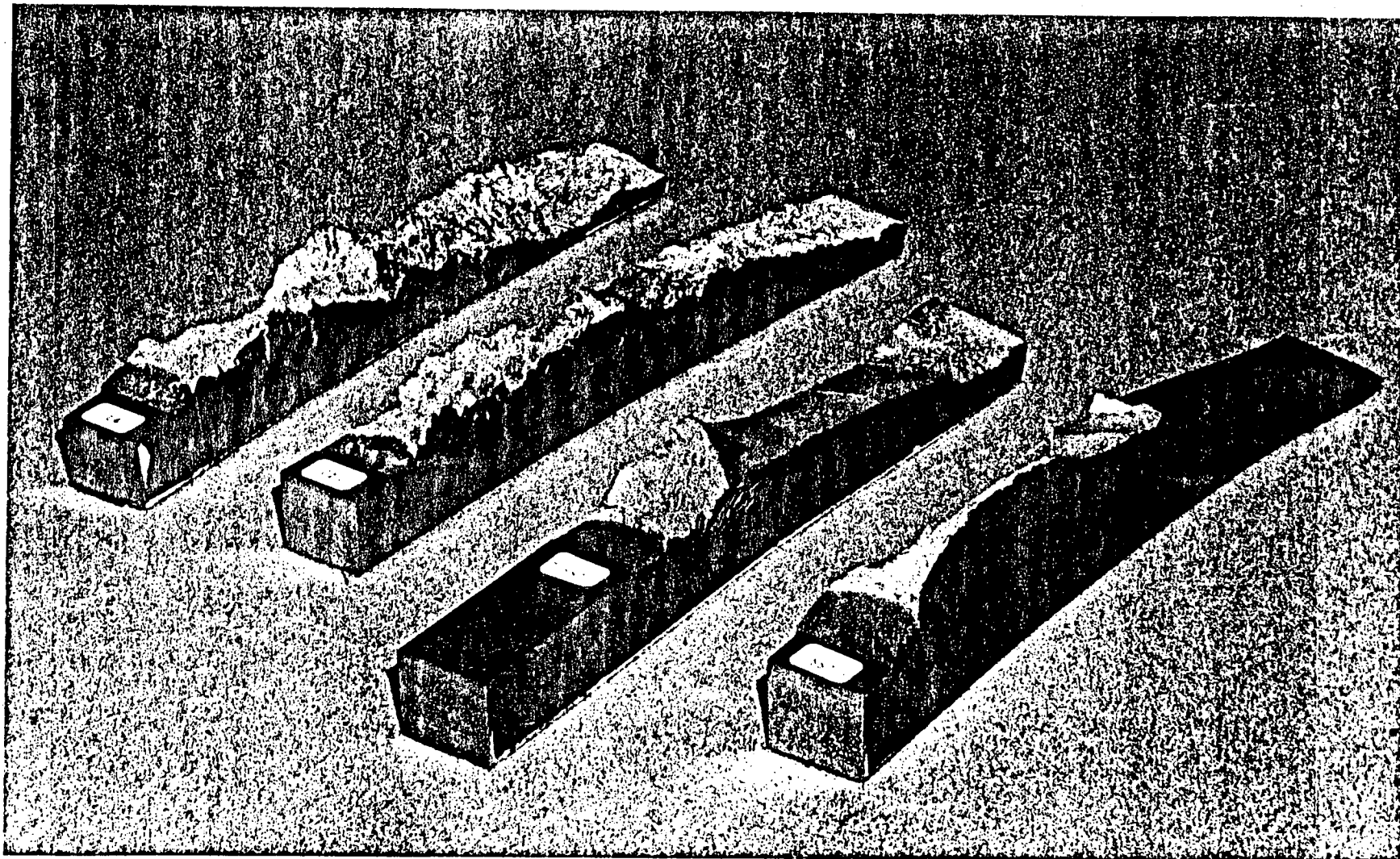


Figure 3 Comparison of Cast CF8M and Wrought A240 Plate Specimens at 550F. Specimens Numbered Left to Right: C4, C2, SS3, SS7

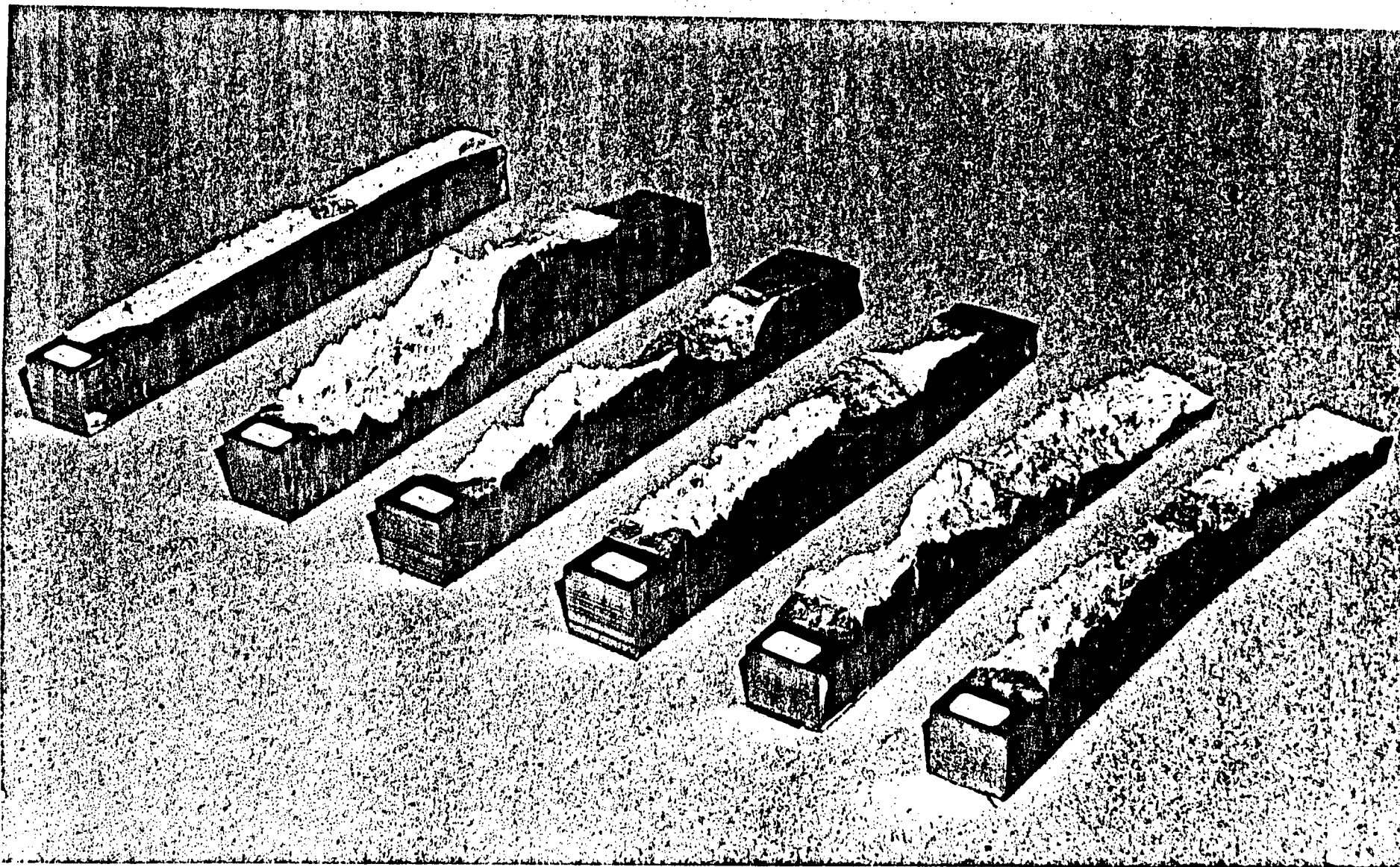


Figure 4 Comparisons of Fracture Surfaces of CF8M Casting Welded with E316L Weld Metal with Base Metal. All Specimens 550F. Specimens Numbered Left to Right: WC1, WC4, WC3, WC2, C4, C2

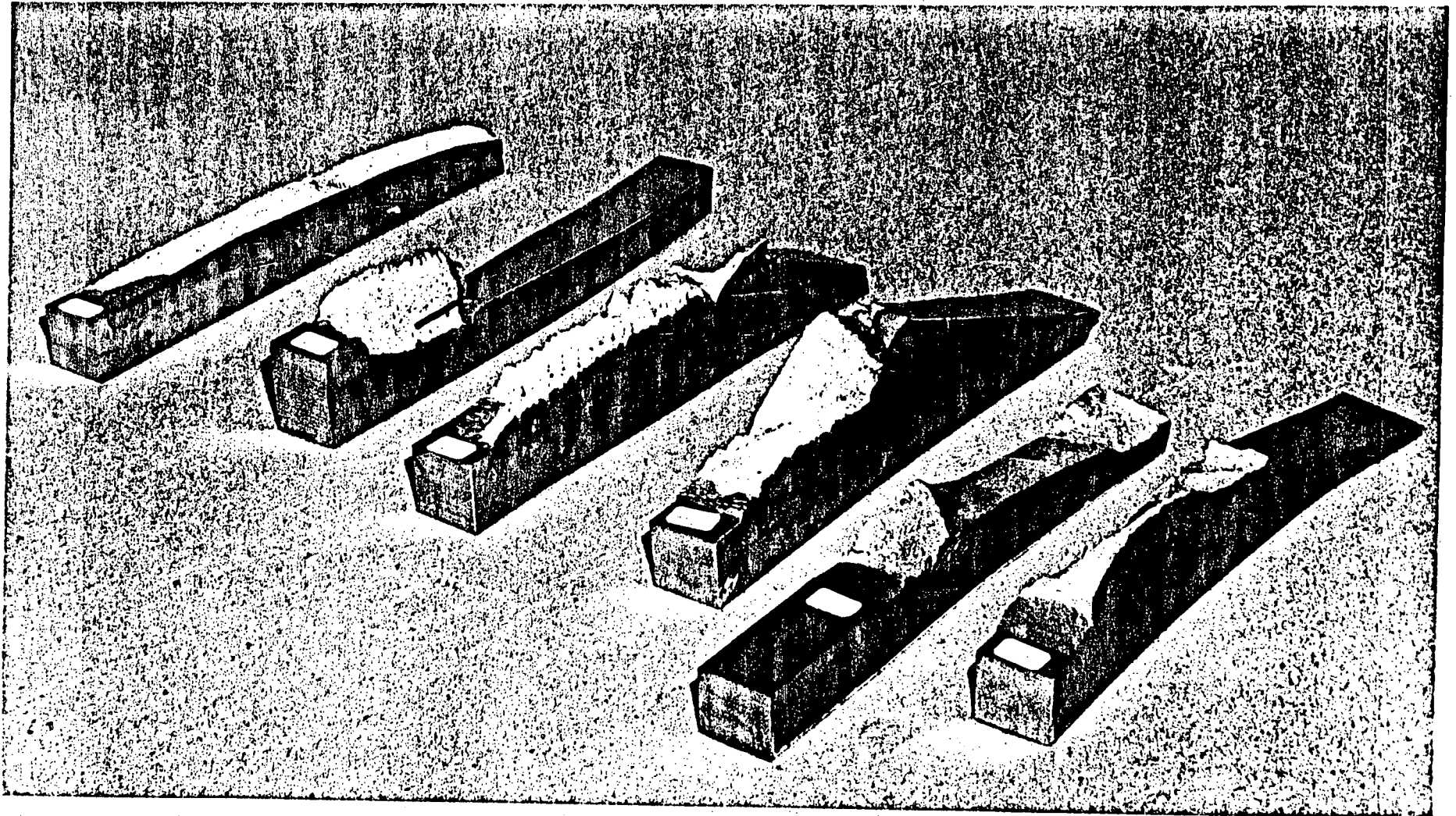


Figure 5 A240 Plate Welded with E316 Electrode Fracture Surfaces Compared with Base Plate for Tests at 550F. Specimens Numbered Left to Right: WSS4, WSS7, WSS6, WSS3, SS3, SS7

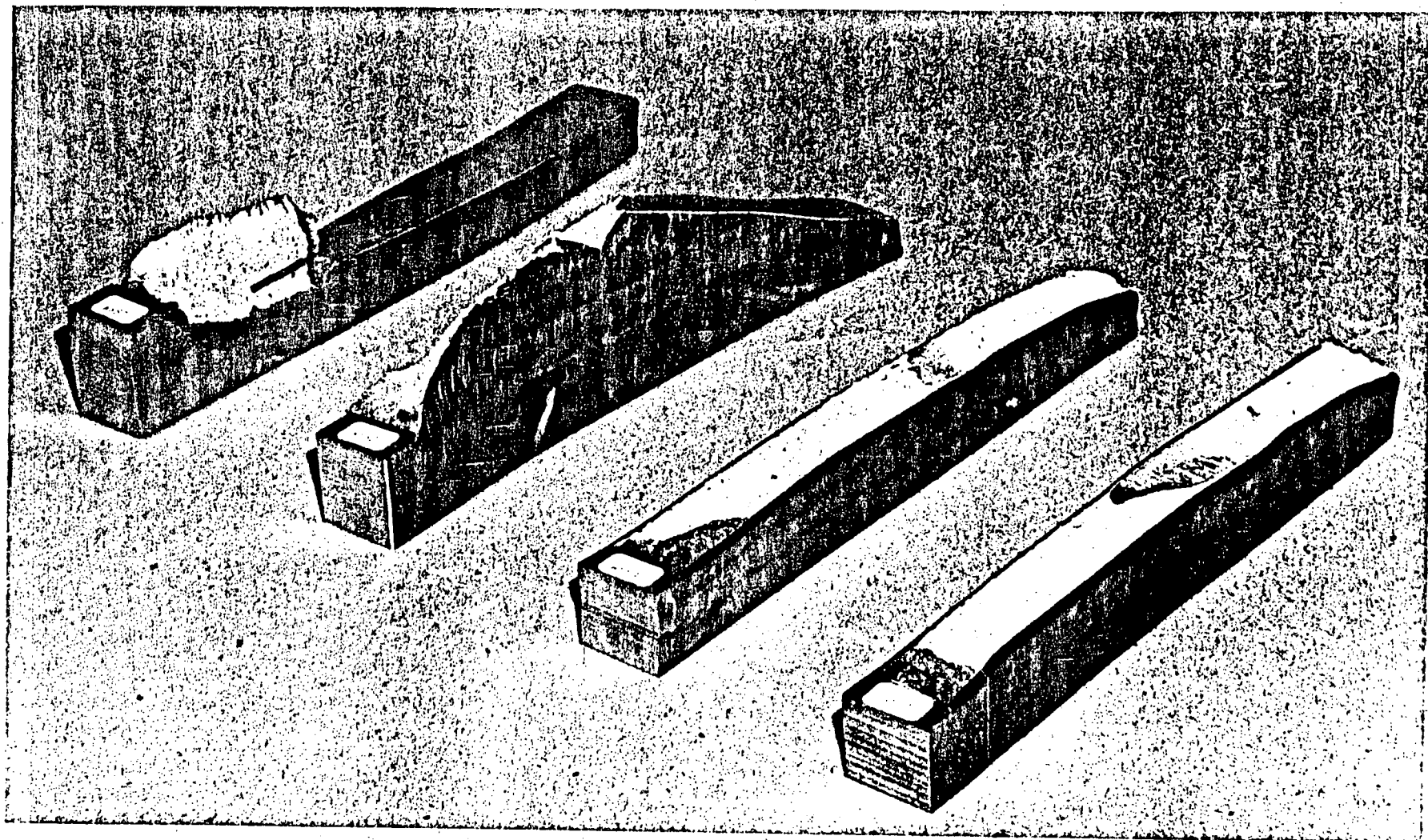


Figure 6 Comparison of the Fracture Surfaces of E316L and Inconel Weld Metal for Specimens Tested at 550F. Numbered Left to Right: WWS7, WSS2, WSS4, WSS1

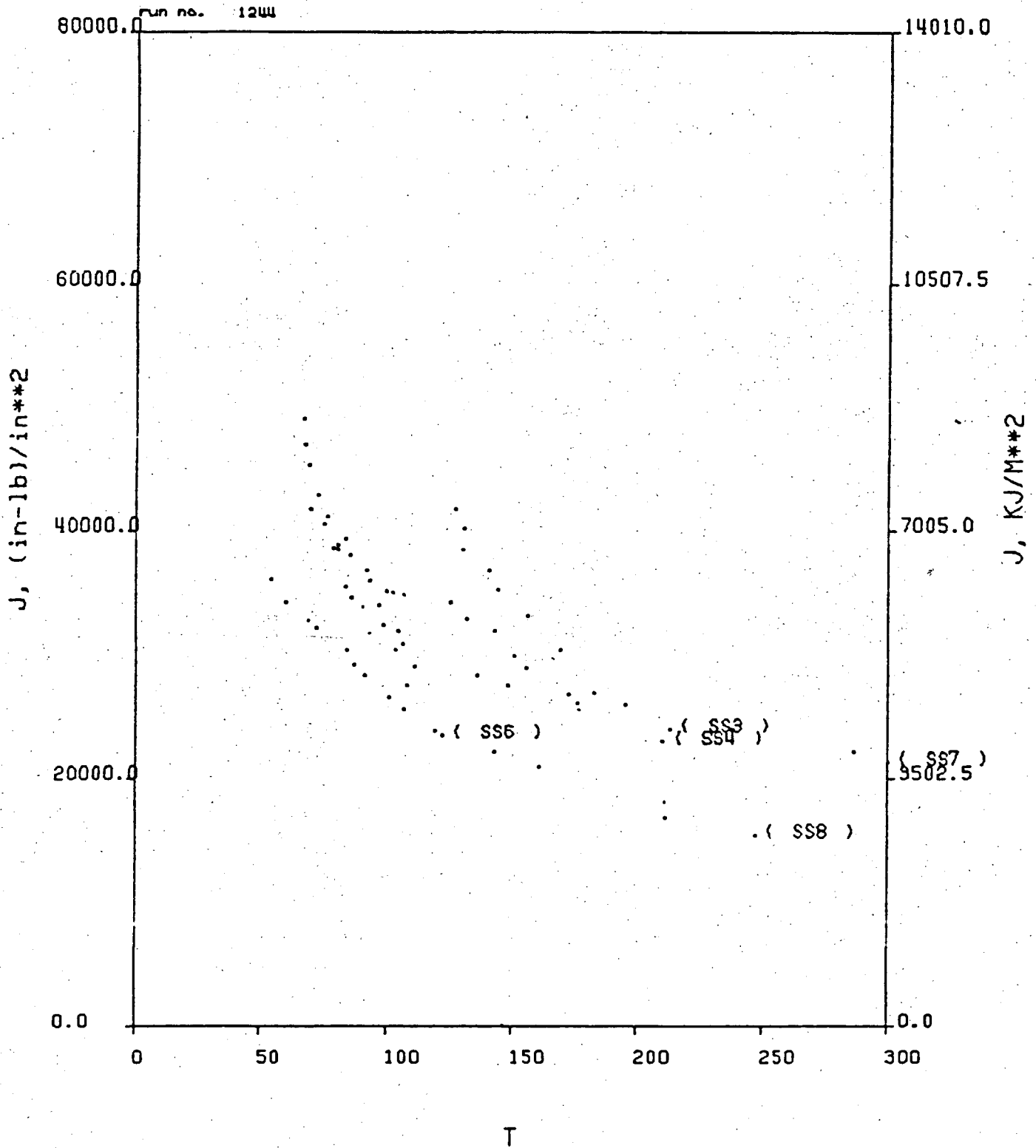


Figure 7 J vs. T Material Curves for A240 Plate at 70F and 550F

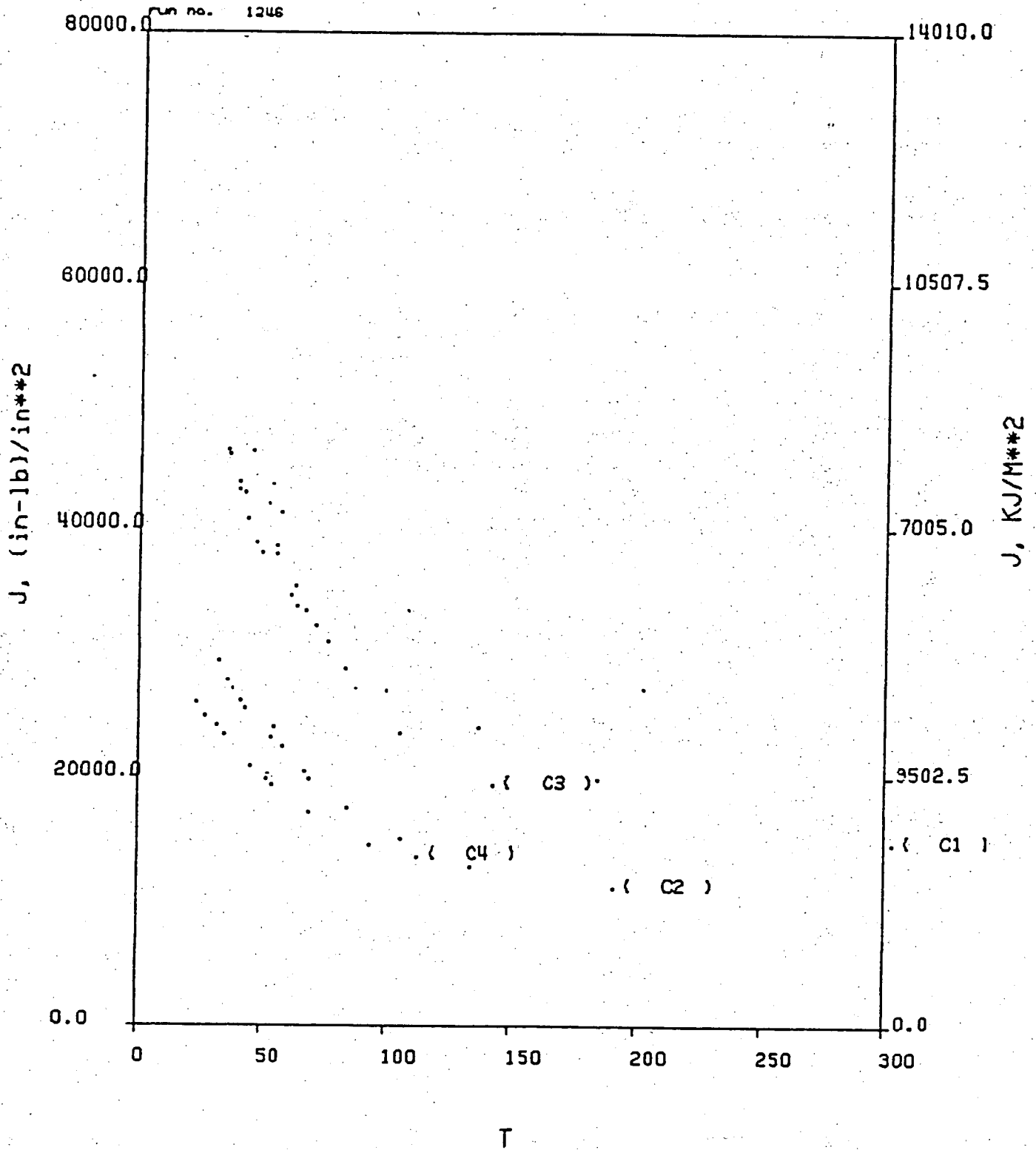


Figure 8 J vs. T Material Curves for CF8M Plate at 70F and 550F

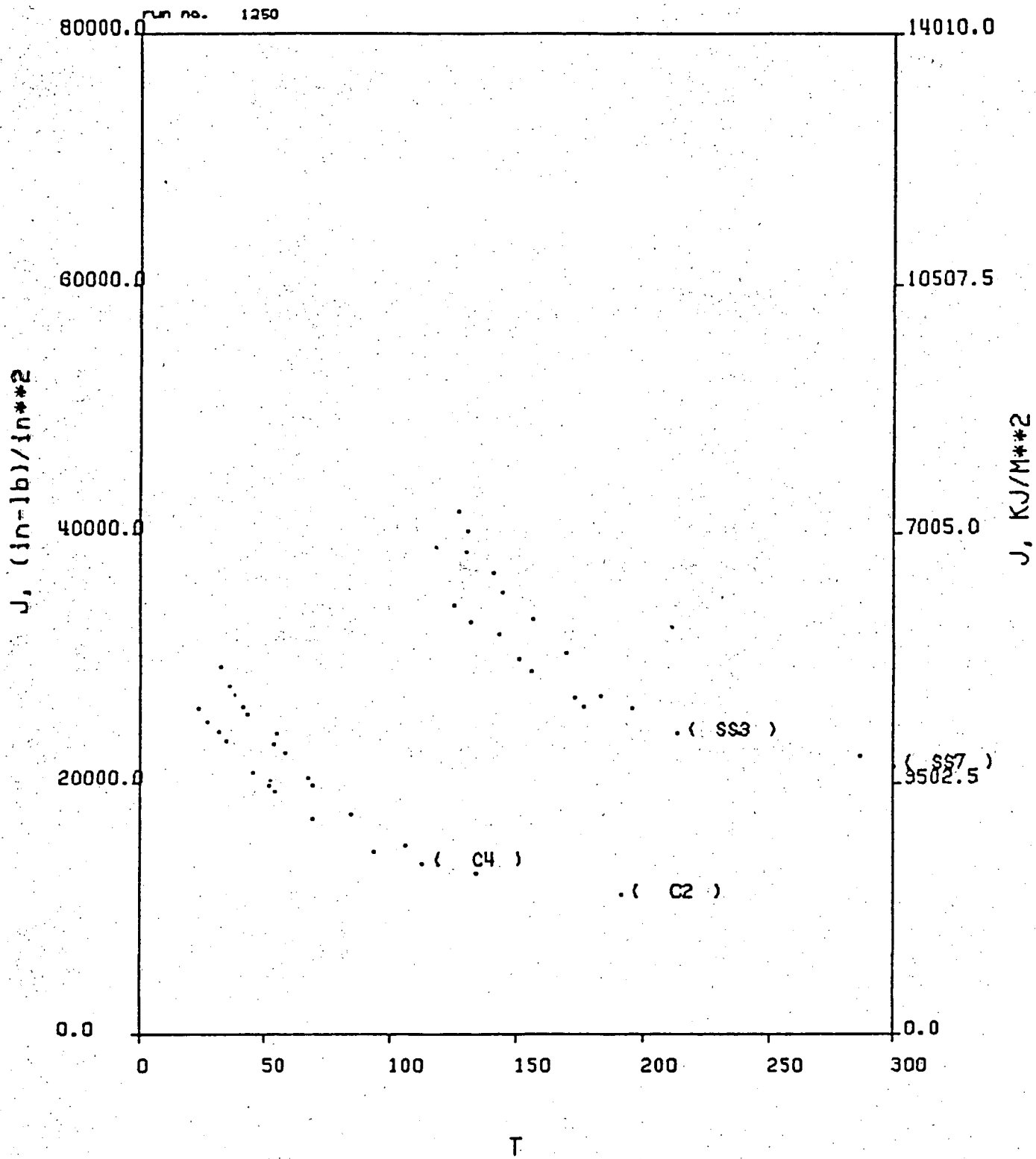


Figure 9 Comparison of J vs. T Material Curves for CF8M Casting with A240 Plate at 550F

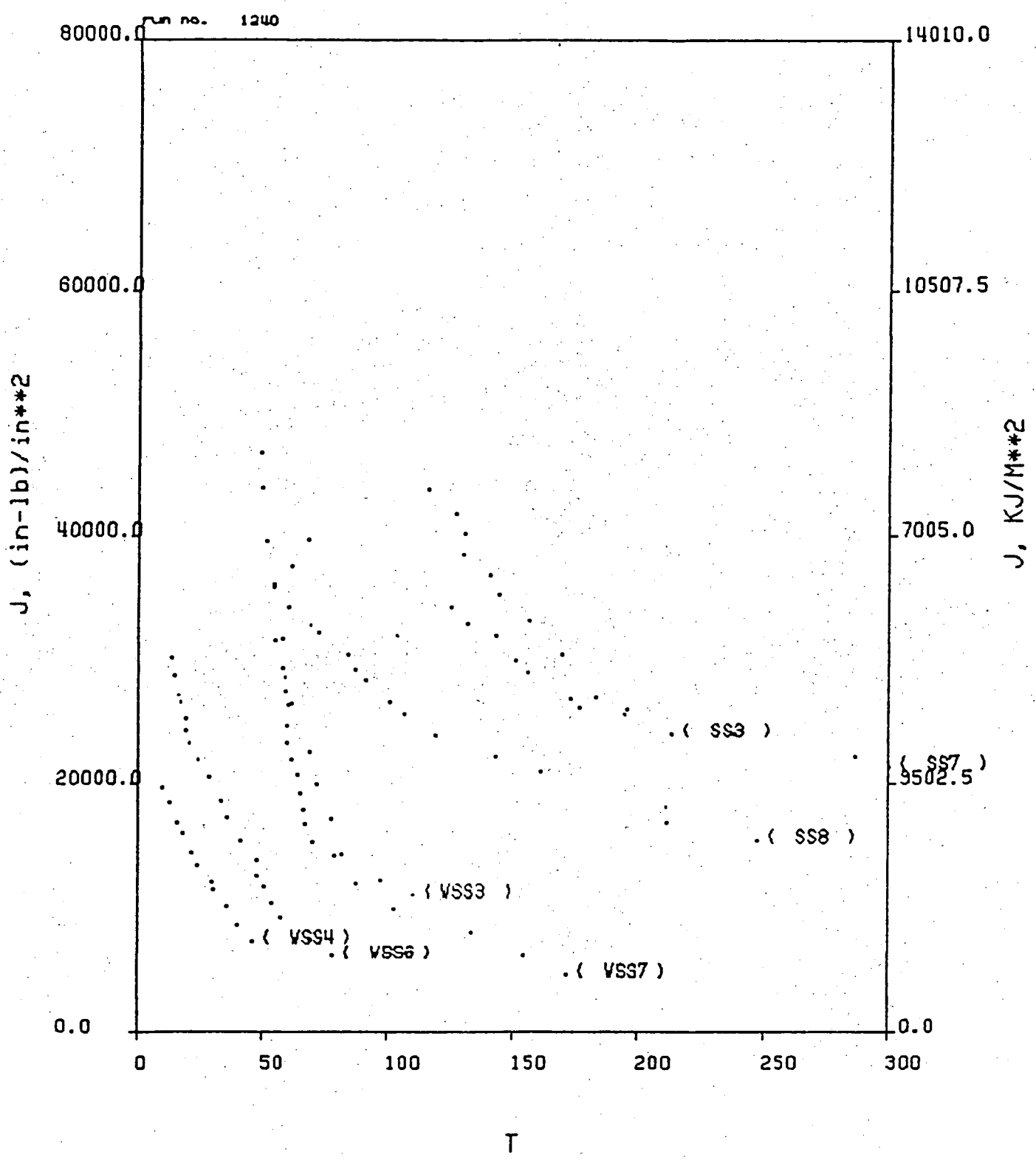


Figure 10 J vs. T Material Curves Comparing Welded A240 Plate with Base Metal at 550F

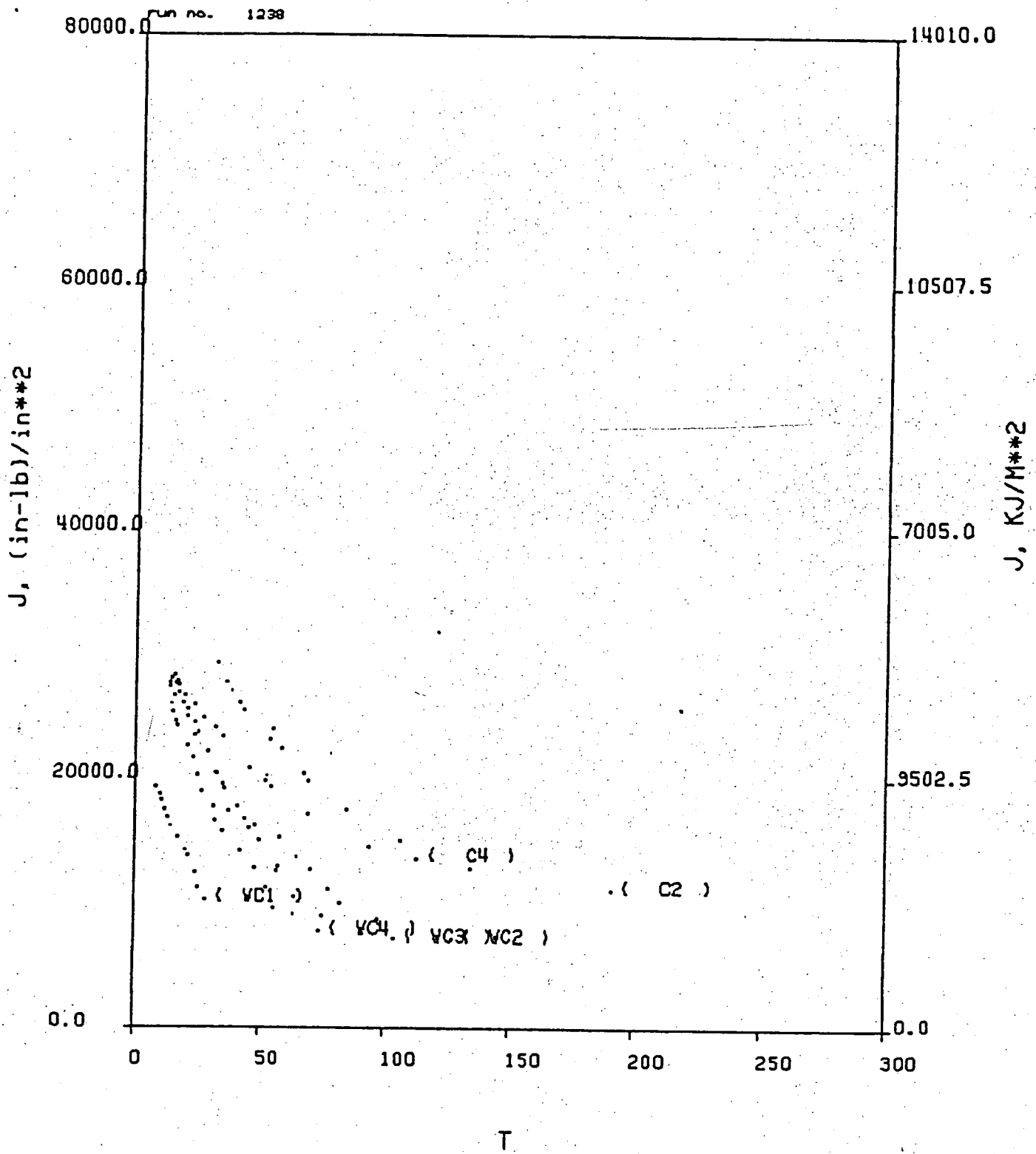


Figure 11 J vs. T Material Curves for E316 Welded CF8M Compared with Base Metal CF8M at 550F

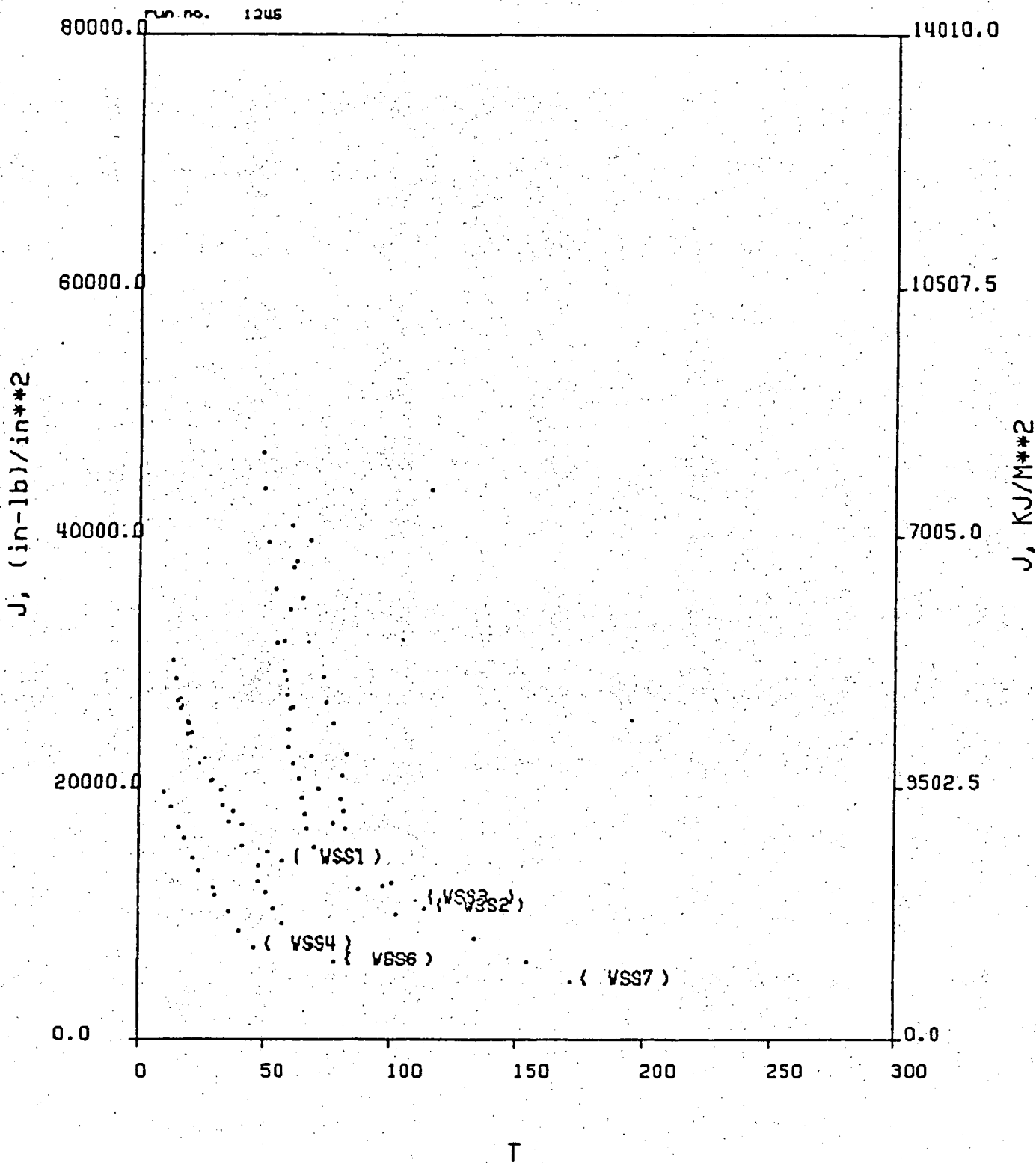


Figure 12 J vs. T Material Curves at 550F Showing Effect of Weld Metal Type and Side-Grooving on Tearing Resistance for Welded A240 Plate

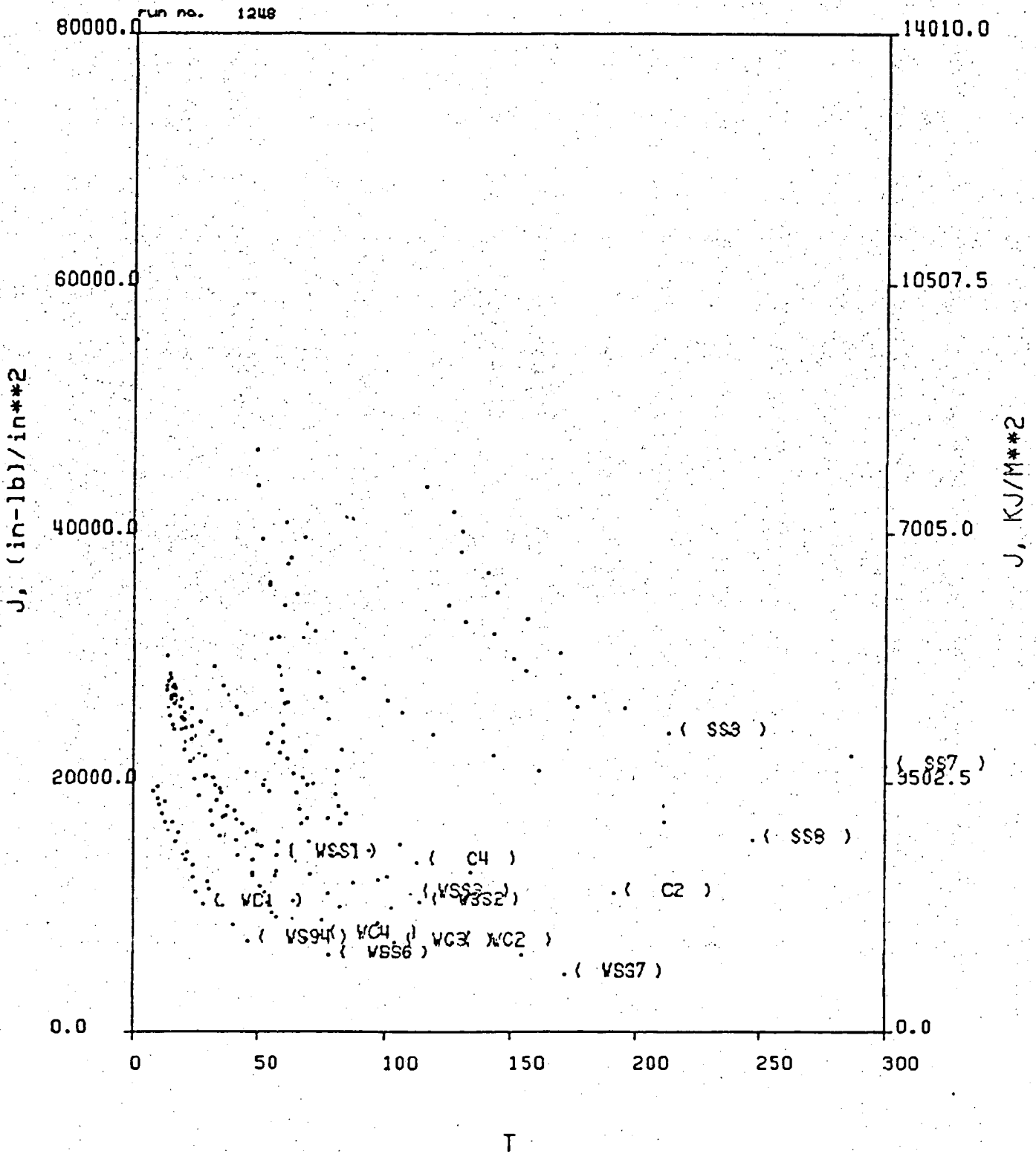


Figure 13 Summary of All J vs. T Data at 550F